Assessing Pediatric Cognitive Development via Multisensory Brain Imaging Analysis

Irina Belyaeva
Department of CSEE
University of Maryland, Baltimore County
Baltimore, MD, USA
irinbel1@umbc.edu

Yu-Ping Wang
Department of Biomedical Engineering
Tulane University
New Orleans, LA, USA
wyp@tulane.edu

Tony W. Wilson
Institute for Human Neuroscience
Boys Town National Research Hospital
Boys Town, NE, USA
tony.wilson@boystown.org

Vince D. Calhoun
Department of Electrical Engineering
Georgia Tech University
Atlanta, GA, USA
vcalhoun@gsu.edu

Julia M. Stephen
Lovelace Biomedical Research Institute
Albuquerque, NM, USA
jstephen@mrn.org

Tülay Adali
Department of CSEE
University of Maryland, Baltimore County
Baltimore, MD, USA
adali@umbc.edu

***Abstract*—Adolescence is a special period between childhood and adulthood and constitutes a critical developmental stage for humans. During adolescence, the brain processes various stimuli to form a complete view of the world. This study highlights the critical role of multisensory integration, where the brain processes multiple senses together rather than focusing on just one sensory modality at a time. Brain imaging modalities such as magnetoencephalography (MEG) and functional magnetic resonance imaging (fMRI) can be utilized to gain insights into the non-additive effects of multisensory integration by fusing data across different sensory stimuli in both time and space. While MEG and fMRI are powerful tools, traditional approaches to combining data from these modalities often ignore their multisensory aspect, focusing instead on single tasks. To leverage their complementarity, we introduce a multitask learning multimodal data fusion framework for joint learning of multisensory brain developmental patterns from MEG and fMRI data through a novel application of coupled canonical polyadic tensor decomposition. The multitask learning paradigm performs multimodal fusion from multiple sensory stimuli using multitask coupled tensor-tensor factorization (MCTTF). We demonstrate that multitask multimodal fusion of MEG and fMRI data can identify unique brain components, demonstrating a higher group-level multisensory integration effect.**

***Index Terms*—coupled tensor-tensor factorization, multimodal data fusion, fMRI, MEG, brain function, multisensory integration, developmental neuroscience**

I. Introduction

Neuroimaging research leverages the capabilities of multitask and multimodal data fusion to explore the complexities of brain functionality and human cognition. Multitask learning, by integrating inputs from multiple senses, significantly improves our understanding of the intricate patterns in brain activity. Adolescence, a period of intense transformation, acts as a bridge from childhood to adulthood, with its rapid developments profoundly influencing developmental trajectory. In this critical developmental stage, multisensory and multimodal neuroimaging has become an essential tool, providing deep insights into the neural bases of cognitive maturation and learning in young populations. However, the complexity and high dimensionality of neuroimaging data pose considerable challenges, necessitating innovative approaches that combine multiple senses and imaging techniques to capture the essence of brain development accurately.

The forefront of multimodal brain imaging analysis is marked by the development of methodologies such as joint independent component analysis [1], coupled matrix/tensor factorization (CMTF) [2], and coupled tensor-tensor factorization (CTTD) [3]. These approaches have shown promising results in extracting and characterizing developmental brain patterns, particularly through the joint analysis of electroencephalography (EEG), magnetoencephalography (MEG) and functional magnetic resonance imaging (fMRI) data using tensor factorizations [4], and in identifying developmental features from pediatric EEG data [5]. Several studies have employed multiway representations and the CMTF-like methods for a comprehensive analysis of neuroimaging data across modalities [4], [6], [7].

Despite these advancements, only a few studies [8], [9] have embraced a multitask approach that not only utilizes multimodality but also encompasses the analysis of multiple paradigms to probe into the intricate details of brain function and structure. This paper introduces a new approach for multitask brain pattern learning through a novel application of coupled canonical polyadic (CP) tensor decomposition [10] via multitask coupled tensor/tensor factorization (MCTTF), specifically designed for the analysis of multisensory and multimodal brain imaging data. By leveraging the power of multimodal tensor fusion, our methodology facilitates simultaneous analysis of multiple sensing and imaging modalities. It captures the complex interactions and inherent multidimensional structure of brain imaging data, allowing for the

This work was supported in part by NSF 2316420, NSF 2112455, NIH R01 MH118695, NIH R01MH123610, NIH R01AG073949, NIH R01 MH121101, and NIH P20 GM14464.

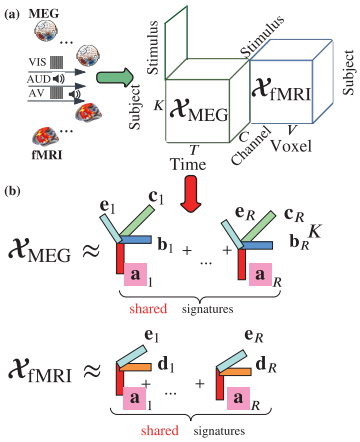

Fig. 1. Multitask generative model for multi-subject MEG and fMRI data via multitask coupled tensor/tensor decomposition. (a) Multitask coupled MEG and fMRI tensor/tensor model. MEG and fMRI tensor formation is achieved by arranging the subject's ERF responses and spatial maps derived from task-related contrast along the subject and stimulus dimension. (b) The MEG and fMRI tensors are decomposed into components, each of which is a rank-1 tensor. Each pattern is characterized by five key signatures: the weight of the subject ($\mathbf{a}_r$), the temporal signature ($\mathbf{b_r}$), the MEG spatial signature ($\mathbf{c_r}$), the fMRI spatial signature ($\mathbf{d_r}$), and the stimulus condition signature ($\mathbf{e_r}$).

exploration of multisensory integration effects (MSI) using tensor-based group-level analysis [4]. This approach offers a novel perspective on the underlying neural mechanisms that support learning and development in children, and enhances the prospective assessment of cognitive development.

II. Multitask Tensor Analysis and Multimodal Fusion of MEG and fMRI Data

A. Multisensory Experimental Paradigm

In our developmental cognitive study [11], participants ($N = 74$) completed a multisensory task during MEG and fMRI scanning, where they were instructed to press their index finger upon seeing, hearing, or both seeing and hearing stimuli. The sensory stimuli (auditory (AUD), visual (VIS), or audio-visual (AV)) were presented for 800 ms each. MEG epochs centered on the stimulus onset were averaged over roughly 100 trials creating sensor-level event-related fields (ERFs) time-locked to the the stimulus condition (AUD, VIS, or AV). In analyzing the fMRI data, stimulus-related three-dimensional (3D) contrast images were computed, temporally aligned to each target stimulus using the general linear model. Participants were categorized into high-performance (HP, n = 38) and low-performance (LP, n = 36) groups based on the outcomes of neuropsychological assessments [4].

B. Generative Model for Multitask Tensor Fusion

We analyzed multitask MEG and fMRI data outlined in Section II-A as a linear mixture of the underlying neural sources. These sources were temporally synchronized across participants within a specific target-related stimulus. It was assumed that these neural sources were represented in both imaging modalities. Our goal was to identify common neural signatures triggered by multisensory stimuli (VIS, AUD, and AV) across subjects. To achieve our objective, we formulated the MCTTF method expanding upon the CMTF [2] and CTTD [3], [10] methods. This development extends these methodologies to a multisensory paradigm, enabling us to simultaneously identify latent brain activity patterns triggered by multiple stimuli. The multimodal data include MEG ERFs, represented as $\boldsymbol{\mathcal{X}}_{\text{MEG}} \in \mathbb{R}^{K\times T\times C\times M}$, and fMRI spatial contrast maps denoted as $\boldsymbol{\mathcal{X}}_{\text{fMRI}} \in \mathbb{R}^{K\times V\times M}$, where K is the number of subjects, T is the number of timepoints, C is the number of MEG sensors, M is the number of stimulus conditions, and V is the number of voxels. These observed multimodal data are modeled using a linear combination of R neural sources: $\boldsymbol{\mathcal{X}}_{\text{MEG}} = \sum_{r=1}^{R} \lambda_r \mathbf{a}_r \circ \mathbf{b}_r \circ \mathbf{c}_r \circ \mathbf{e}_r$, $\boldsymbol{\mathcal{X}}_{\text{fMRI}} = \sum_{r=1}^{R} \sigma_r \mathbf{a}_r \circ \mathbf{d}_r \circ \mathbf{e}_r$, where $\mathbf{a}_r \in \mathbb{R}^K$ indicates the assignment of subject weights to the rth source across K subjects. The terms λ_r and σ_r denote normalization weights with a 2-unit norm for the MEG and fMRI modalities, respectively. The vector $\mathbf{b}_r \in \mathbb{R}^T$ reflects the temporal activity of the rth source different timepoints T. Similarly, $\mathbf{c}_r \in \mathbb{R}^C$ captures the spatial source activity across different MEG sensors C. The spatial sensitivity for fMRI contrast maps is captured by $\mathbf{d}_r \in \mathbb{R}^V$. Lastly, the vector $\mathbf{e}_r \in \mathbb{R}^M$, signifies the contribution of the mth stimulus condition on the rth source. Fig. 1a illustrates the generative model designed for the multimodal data fusion of multitask data from MEG and fMRI recordings. In this model, the MEG data is represented as a 4D tensor, while the fMRI data is captured in a 3D tensor. The data fusion of MEG and fMRI data is achieved through their coupling along the common subject dimension.

C. Multitask Joint Tensor Factorization

The MCTTF for the generative model shown in Fig. 1 can be written as

$$\begin{aligned} f(\boldsymbol{\Lambda},\boldsymbol{\Sigma},\mathbf{A},\mathbf{B},\mathbf{C},\mathbf{D},\mathbf{E}) = \\ \min_{\boldsymbol{\Lambda},\boldsymbol{\Sigma},\mathbf{A},\mathbf{B},\mathbf{C},\mathbf{D},\mathbf{E}} \frac{1}{2}\|\boldsymbol{\mathcal{X}}_{\text{MEG}} - [[\boldsymbol{\Lambda},\mathbf{A},\mathbf{B},\mathbf{C},\mathbf{E}]]\|_F^2 \\ + \frac{1}{2}\|\boldsymbol{\mathcal{X}}_{\text{fMRI}} - [[\boldsymbol{\Sigma},\mathbf{A},\mathbf{D},\mathbf{E}]]\|_F^2, \\ \text{s.t. } \|\mathbf{a}_r\|_2 = \|\mathbf{b}_r\|_2 = \|\mathbf{c}_r\|_2 = \|\mathbf{d}_r\|_2 = \|\mathbf{e}_r\|_2 = 1, \end{aligned} \quad (1)$$

where $\|\cdot\|_F$ denotes the Frobenius norm, $\mathbf{a}_r \in \mathbb{R}^K, \mathbf{b}_r \in \mathbb{R}^T, \mathbf{c}_r \in \mathbb{R}^C, \mathbf{d}_r \in \mathbb{R}^V, \mathbf{e}_r \in \mathbb{R}^M$, are the columns of the factor matrices $\mathbf{A}$, $\mathbf{B}$, $\mathbf{C}$, $\mathbf{D}$, $\mathbf{E}$ normalized to a 2-unit norm for $r = 1, \cdots, R$. The norms are absorbed into diagonal matrices $\boldsymbol{\Lambda} \in \mathbb{R}^{R\times R}$, $\boldsymbol{\Sigma} \in \mathbb{R}^{R\times R}$. The matrices $\mathbf{A} \in \mathbb{R}^{K\times R}$, $\mathbf{B} \in \mathbb{R}^{T\times R}, \mathbf{C} \in \mathbb{R}^{C\times R}$, $\mathbf{D} \in \mathbb{R}^{V\times R}$, $\mathbf{E} \in \mathbb{R}^{M\times R}$ correspond to the factor matrices in the subject, time, sensor, voxel and stimulus modes. This approach facilitates the assessment of non-additive effects in the MSI and enables the investigation of the relationship between MEG ERF and fMRI spatiotemporal brain activation patterns [4].

III. Experiments

A. Multitask Component Extraction

The MEG ERFs and fMRI spatial contrast maps were transformed into data tensors, with the MEG ERFs being

organized into a 4D tensor denoted by $\boldsymbol{\mathcal{X}}_{\text{MEG}} \in \mathbb{R}^{K\times T\times C\times M}$, and the fMRI data into a 3D tensor represented as $\boldsymbol{\mathcal{X}}_{\text{fMRI}} \in \mathbb{R}^{K\times V\times M}$. This was achieved by arranging the subject ERFs $\mathbf{S}_k \in \mathbb{R}^{C\times T}$, and the spatial maps from fMRI, $\mathbf{s}_k \in \mathbb{R}^{V}$, into a multidimensional structure where each dataset was stacked across subject and stimulus condition modes. We conducted MCTTF with a tensor rank R, identified using the core consistency diagnostic (CCD) [12], and the average congruence product (ACP) [13]. We selected the model with the highest CCD and ACP values when evaluated for values of tensor rank $R = 1, \cdots, 10$. The fitted MCTTF model resulted in the R-component factor matrices $\mathbf{A}$, $\mathbf{B}$, $\mathbf{C}$, $\mathbf{D}$, $\mathbf{E}$ that were used to reconstruct joint group-level MEG ERF and fMRI latent components for each stimulus condition (VIS, AUD, and AV).

B. Statistical Analysis of Multisensory Integration

To examine the group-level MSI effect using MCTTF, we calculated the SUM:(AUD + VIS) and DIFF: [AV − (AUD + VIS)] stimulus types for each rth latent component, yielding in R components for the SUM and DIFF stimulus types. The components for the SUM and DIFF stimulus types represent a linear combination of the estimated condition weights for the AUD, VIS, and AV conditions found in the estimated factor matrix $\mathbf{E} \in R^{M\times R}, m = 1, \cdots 3$. The multisensory integration effect was analyzed by examining the differences between multisensory and additive stimulus (AV vs. SUM) within each component and subject group (HP vs. LP). Statistically significant differences in the facilitation measure [AV − (AUD + VIS)] indicated multisensory facilitation, thereby suggesting a physiological benefit from multisensory integration [14].

IV. Results

The MCTTF method (1) was employed to extract joint MEG ERF and fMRI components. This was followed by a statistical assessment to identify the effects of the group-level multisensory facilitation. The estimation of factor matrices for the MCTTF model utilized the coupled CP Alternating Least Squares (CP-ALS) method [10]. To ensure the reliability of the model, it was fitted 100 times with random initialization, from which the most stable iteration was selected for further analysis. The stability analysis indicated that all runs at a fixed R yielded similar the residual mean square values (RMSE), with a standard error of the mean (SEM) of < 0.001. The final model order was determined by the highest ACP and CCD values across MEG and fMRI modalities, which resulted in the lowest SEM for the RMSE metric. Consequently, a tensor rank of 4 ($R = 4$) was selected for the MCTTF.

A. Multisensory Tensor Analysis of Multitask MEG and fMRI Data Using MCTTF Model

In the tensor analysis employing the MCTTF model (1), a total of 12 joint components were extracted across VIS, AUD, and AV conditions. These components were characterized by their major ERFs peaks and functional fMRI activations. We show the joint components obtained from the MCTTF decomposition for the audio-visual condition

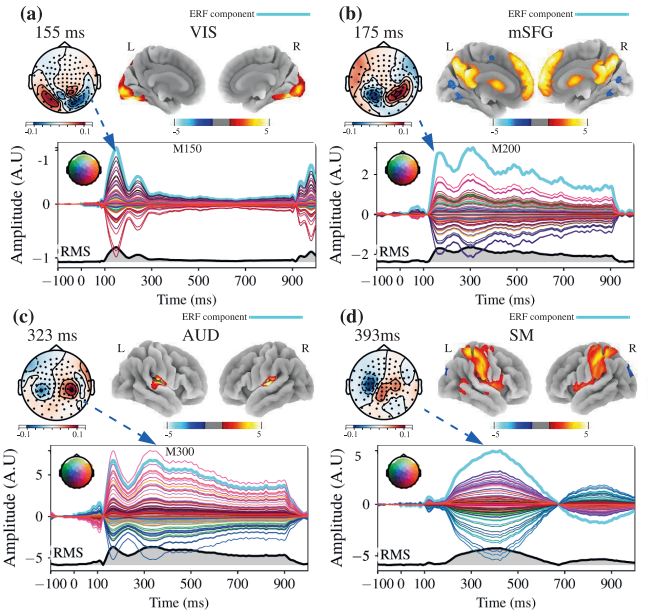

Fig. 2. Group averaged results of the MCTTF MEG and fMRI decomposition for the AV stimulus. Each identified joint component is depicted through the ERF component and a corresponding fMRI component. (a) Joint VIS/M150 component. (b) Joint mSFG/M200 component. (c) Joint AUD/M300 component. (d) Joint SM/M400 component. VIS: visual, mSFG: superior frontal gyrus (medial part), AUD: auditory, SM: sensorimotor.

in Fig. 2, which had the most prominent brain patterns. Each subfigure within Fig. 2 presents the fMRI component activations and their corresponding ERF component. The ERF components illustrate signal traces from all individual MEG sensors, averaged across subject ERF components, with the mean ERF component (averaged across sensors) depicted in cyan. A visual component (VIS/M150) was identified with an initial prominent peak at 150–155 ms shown in Fig. 2a. A nonparametric permutation t-test (one-tailed, thresholded at $p < 0.05$) revealed corresponding fMRI activation in the bilateral cuneus (CUNC.L/R, Brodman Area (BA) 19), fusiform gyrus (FFG.R, BA37), and lingual gyrus (LING.R, BA18). The prefrontal mSFG/M200 component characterized by an early peak at around 82 ms and a second peak at 175 ms is shown in Fig. 2b. The fMRI activation areas corresponding to the mSFG/M200 component were located in the medial superior frontal gyrus (mSFG, BA9) and the precuneus (PCUN, BA7). The auditory AUD/M300 component is shown in Fig. 2c peaked at about 105–110 ms, and 310–323 ms. The associated fMRI activations for the AUD/M300 component were found in the bilateral superior temporal gyrus (STG.L/R, BA22) and the bilateral Heschl's gyrus (HES.L/R, BA41/42). The sensorimotor SM/M400 component shown in Fig. 2d was characterized by early sensory subcomponents occurring at approximately 100–110 ms, alongside a late latency subcomponent at around 390–400 ms. The fMRI activations within the SM/M400 component were observed in the secondary somatosensory cortex (bilateral postcentral gyrus (Post.CG.L/R, BA1/2/3)) and in the primary motor cortex (the bilateral precentral gyrus (Pre.CG.L/R, BA4)).

B. Statistical Group-level Analysis of Multisensory Integration Effects

1) Group-level Sensitivity Analysis of Multisensory Facilitation: In this section, we present the group-level sensitivity analyses outlined in Section III-B. The purpose of the analyses is to evaluate the extent of multisensory facilitation from the multisensory stimulus (AV), in contrast to the linear sum of the AUD and VIS stimuli, termed as SUM stimulus: (AUD + VIS). Additionally, we examine the differences in multisensory gain measure ([AV − (AUD + VIS)]) between groups (HP vs. LP). A three-way mixed-design ANOVA was conducted to quantify the multisensory facilitation effect. The subject group (HP vs. LP) served as the between-subjects factor, while component (VIS/M150, mSFG/M200, AUD/M300, and SM/M400) and stimulus type (AV vs. SUM) were within-subjects factors. The results revealed a significant interaction between stimulus type and group for the VIS/M150 ($F_{1,144} = 12.0, p < 0.001, \eta_G^2 = 0.08$) and SM/M400 ($F_{1,144} = 43.01, p < 0.001, \eta_G^2 = 0.23$) components, indicating differential multisensory facilitation for these components between groups. No significant interaction was found for mSFG/M200 and AUD/M300 components. Fig. 3a illustrates the main effects of the multisensory enhancement (AV vs. SUM) across these components.

Following the significant interaction, post-hoc two-tailed t-tests (the false discovery rate (FDR) corrected, $p < 0.05$) assessed differences in multisensory gain (DIFF: [AV − (AUD + VIS)]) between groups for each component. These tests revealed significant group differences (HP vs. LP) for VIS/M150 ($t_{74} = 5.92$) and SM/M400 ($t_{74} = 9.51$) components, indicating stronger multisensory facilitation in the HP group (see Fig. 3b). Fig. 4 presents group-level discriminative components with significant multisensory facilitation effect (AV vs. AUD + VIS) for the VIS/M150 component within each group (HP and LP). The results demonstrate multisensory facilitation occurring at approximately 269 ms (Fig. 4a–b). The thresholded group-level two-tailed T-maps ($p < 0.05$), shown in Fig. 4c, indicate significant activity in the middle and superior occipital gyri (MOG/BA18 and SOG/BA19), as well as in the PCUN/BA7 and FFG/BA37. Notably, the HP group demonstrated stronger facilitation in these regions compared to the LP group. Furthermore, significant multisensory facilitation was observed for the SM/M400 component, with stronger activation in the HP group compared to the LP group ($p < 0.001$) peaking at around 240 ms. This activation involved brain areas such as the superior parietal gyrus (SPG/BA7), the secondary somatosensory cortex (Post.CG.L/R, BA1/2/3), and the right insula (INS.R, BA13).

2) Multisensory Facilitation and Cognitive Performance: We investigated the association between multisensory gain and cognitive performance in the full sample ($N = 74$). Discriminative multisensory components, VIS/M150 and SM/M400, were correlated with nine age-adjusted neuropsychological (T) scores. Two-tailed Pearson's correlation tests with FDR correction ($p < 0.05$) revealed significant associations between discriminative components and specific cognitive do-

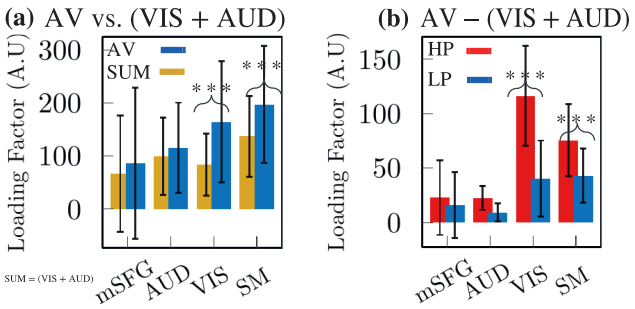

Fig. 3. Main effect of the multisensory facilitaion ($N = 74$) estimated by MCTTF method: AV vs. SUM: [(VIS + AUD)]. The boxplots summarize the distribution of the mean component loading factors for the AV and SUM stimilus type for the VIS, AUD, mSFG and SM components. The error bars represent the standard error of the mean. Post hoc analyses with two tailed t-tests (FDR corrected, $p < 0.05$) indicate that the mean of the components extracted from the mutisensory AV condition was significantly higher than of those computed using the SUM stimilus type. (***: $p < 0.001$).

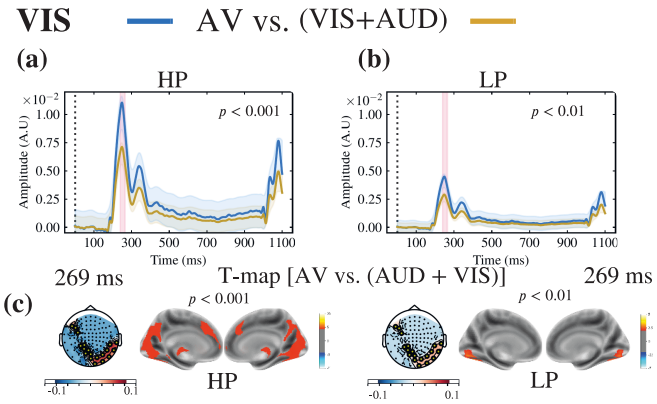

Fig. 4. Group-level discriminative components with significant multisensory facilitation effect for the VIS/M150 component. (a)–(b) HP (left) and LP (right) AV and SUM [(AUD + VIS)] components averaged across all sensors. Time interval of significant difference between stimuli (AV vs. SUM) (240–272 ms) is indicated by the pink region between AV and SUM components. (c) Group-level T-maps ($p < 0.05$) of the DIFF component [AV − (AUD + VIS)] show the multisensory gain in the bilateral CUN (BA19), PCUN (BA7), and FFG gyri (BA37).

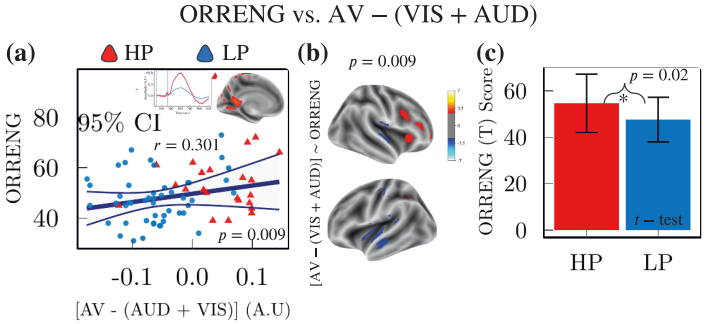

Fig. 5. Significant (FDR corrected, $p < 0.05$) two-tailed partial Pearson's correlations (correlation coefficient, r) between the SM/400 component extracted from the DIFF stimulus and ORRENG (T) score in the full ($N = 74$) sample. The linear fit and 95% confidence intervals (CIs) are shown. (a) The SM/400 component was positively correlated with the ORRENG (T) score. (b) MANCOVA Z-maps ($p < 0.05$) show brain regions of discriminative SM/400 component significantly correlated with ORRENG (T) score. (c) Significant main effect of subject group on ORRENG (T) score ($p < 0.05$).

mains. The SM/M400 component showed a positive correlation with the ORRENG (T) score (language comprehension) ($r_{\mathrm{SM/M400}}(74) = 0.301, p = 0.009$). Conversely, the VIS/M150 component had a negative correlation with the Inattention score ($r_{\mathrm{VIS/M150}}(74) = -0.274, p = 0.02$). Fig. 5a depicts the significant association of the SM/M400 component with the ORRENG (T) score in the full sample. Furthermore, a multivariate analysis of covariance (MANCOVA) was conducted to identify brain regions associated with the significant cognitive domains. MANCOVAs generated voxel-wise associations between fMRI components and cognitive scores, which are shown as Z-maps (FDR corrected, $p < 0.05$). Follow-up MANCOVAs for the SM/M400 component and ORRENG (T) score revealed positive activations (see Fig. 5b) in the right insular cortex (INS.R/BA13) and right inferior frontal gyrus (triangular part) (IFG.R/BA10/45/46). These findings align with the ORRENG t-tests between participant groups (HP vs. LP) shown in Fig. 5c, where the HP group demonstrated better performance compared to the LP group. Finally, the MANCOVA for the VIS/M150 component revealed negative associations with the superior frontal gyrus (SFG/BA32/10/11).

V. Discussion and Conclusion

In this study, we introduced the MCTTF method as a novel approach for the analysis of multitask patterns, specifically designed to analyze multisensory data from both MEG and fMRI within multimodal data fusion. We utilized the MCTTF (1) to investigate the neural correlates of MSI by comparing responses to multisensory stimulus AV and the additive sum of responses to unisensory stimuli (AUD + VIS). Analyzing the AV condition alone cannot differentiate between response differences due to inherent unisensory variations and true multisensory processing. Therefore, the comparison with the SUM stimulus isolates components specific to multisensory integration. Through this comparative analysis, we were able to identify specific sensory and sensorimotor components, which were pinpointed differences in mid-latency at about 240–270 ms located in the higher visual cortices and in the secondary somatosensory brain regions. Furthermore, group-level analysis of MSI integration revealed a higher multisensory gain in the HP group compared to the LP group. These findings align with observed differences in cognitive performance and multisensory facilitation and are consistent with existing literature on adolescent MSI research [15], [16]. Additionally, we identified significant correlations between discriminative components and specific cognitive domains. Notably, the language domain correlated with activity in the right insular cortex, a region recognized as a key hub during multisensory integration [17], [18]. This research highlights the potential of MCTTF for investigating complex multisensory processes. Our findings provide novel insights into the neural mechanisms underlying MSI, demonstrating its sensitivity to individual cognitive differences and its potential influence on cognitive performance. The MCTTF method offers a powerful tool for future investigations into the complex dynamics of multisensory processing in the brain, setting the stage for further exploratory efforts to study cognitive functions in adolescent cohorts.

References

[1] V. D. Calhoun *et al.*, "Neuronal chronometry of target detection: fusion of hemodynamic and event-related potential data," *Neuroimage*, vol. 30, no. 2, pp. 544–553, 2006.

[2] E. Acar, E. E. Papalexakis, G. Gürdeniz, M. A. Rasmussen, A. J. Lawaetz, M. Nilsson, and R. Bro, "Structure-revealing data fusion," *BMC bioinformatics*, vol. 15, no. 1, pp. 1–17, 2014.

[3] C. Chatzichristos *et al.*, "Early soft and flexible fusion of electroencephalography and functional magnetic resonance imaging via double coupled matrix tensor factorization for multisubject group analysis," *Human brain mapping*, vol. 43, no. 4, pp. 1231–1255, 2022.

[4] I. Belyaeva, B. Gabrielson, Y.-P. Wang, T. W. Wilson, V. D. Calhoun, J. M. Stephen, and T. Adali, "Learning spatiotemporal brain dynamics in adolescents via multimodal MEG and fMRI data fusion using joint tensor/matrix decomposition," *IEEE Transactions on Biomedical Engineering*, 2024.

[5] E. Kinney-Lang *et al.*, "Introducing the joint EEG-development inference (JEDI) model: A multi-way, data fusion approach for estimating paediatric developmental scores via EEG," *IEEE transactions on neural systems and rehabilitation engineering*, vol. 27, no. 3, pp. 348–357, 2019.

[6] Y. Jonmohamadi *et al.*, "Extraction of common task features in EEG-fMRI data using coupled tensor-tensor decomposition," *Brain Topography*, vol. 33, no. 5, pp. 636–650, 2020.

[7] E. Acar, *et al.*, "Unraveling diagnostic biomarkers of schizophrenia through structure-revealing fusion of multi-modal neuroimaging data," *Frontiers in neuroscience*, vol. 13, p. 416, 2019.

[8] Y. Zhang, L. Xiao, G. Zhang, B. Cai, J. M. Stephen, T. W. Wilson, V. D. Calhoun, and Y.-P. Wang, "Multi-paradigm fMRI fusion via sparse tensor decomposition in brain functional connectivity study," *IEEE journal of biomedical and health informatics*, vol. 25, no. 5, pp. 1712–1723, 2020.

[9] Y. Bai, Y. Gong, J. Bai, J. Liu, H.-W. Deng, V. Calhoun, and Y.-P. Wang, "A joint analysis of multi-paradigm fMRI data with its application to cognitive study," *IEEE transactions on medical imaging*, vol. 40, no. 3, pp. 951–962, 2020.

[10] M. Sørensen and L. D. De Lathauwer, "Coupled canonical polyadic decompositions and (coupled) decompositions in multilinear rank-(l_r,n,l_r,n,1) terms—part I: Uniqueness," *SIAM Journal on Matrix Analysis and Applications*, vol. 36, no. 2, pp. 496–522, 2015.

[11] J. M. Stephen *et al.*, "The developmental chronnecto-genomics (DevCoG) study: A multimodal study on the developing brain," *NeuroImage*, vol. 225, p. 117438, 2021.

[12] R. Bro and H. A. Kiers, "A new efficient method for determining the number of components in PARAFAC models," *Journal of Chemometrics: A Journal of the Chemometrics Society*, vol. 17, no. 5, pp. 274–286, 2003.

[13] G. Tomasi and R. Bro, "PARAFAC and missing values," *Chemometrics and Intelligent Laboratory Systems*, vol. 75, no. 2, pp. 163–180, 2005.

[14] S. Molholm, W. Ritter, M. M. Murray, D. C. Javitt, C. E. Schroeder, and J. J. Foxe, "Multisensory auditory–visual interactions during early sensory processing in humans: a high-density electrical mapping study," *Cognitive brain research*, vol. 14, no. 1, pp. 115–128, 2002.

[15] A. B. Brandwein, J. J. Foxe, N. N. Russo, T. S. Altschuler, H. Gomes, and S. Molholm, "The development of audiovisual multisensory integration across childhood and early adolescence: a high-density electrical mapping study," *Cerebral cortex*, vol. 21, no. 5, pp. 1042–1055, 2011.

[16] R. J. Alghamdi, M. J. Murphy, N. Goharpey, and S. G. Crewther, "The age-related changes in speed of visual perception, visual verbal and visuomotor performance, and nonverbal intelligence during early school years," *Frontiers in Human Neuroscience*, vol. 15, p. 667612, 2021.

[17] T. Chen, L. Michels, K. Supekar, J. Kochalka, S. Ryali, and V. Menon, "Role of the anterior insular cortex in integrative causal signaling during multisensory auditory–visual attention," *European Journal of Neuroscience*, vol. 41, no. 2, pp. 264–274, 2015.

[18] D. Brunert and M. Rothermel, "Cortical multisensory integration—a special role of the agranular insular cortex?" *Pflügers Archiv-European Journal of Physiology*, vol. 472, no. 6, pp. 671–672, 2020.